$2n-90-CR$

238

(NASA-TM-893410)   THE PULSATIONS OF MODELS   N90-70535
OF DELTA CEPHEI STARS, 2   (NASA)   23 p

                                                    Unclas
                                          00/90   0266107

THE PULSATIONS OF MODELS OF DELTA CEPHEI STARS. II

NORMAN BAKER*

Department of Physics, New York University, and Institute for Space Studies
Goddard Space Flight Center, NASA, New York

AND

RUDOLF KIPPENHAHN†

Max-Planck-Institut für Physik und Astrophysik, Munich

ABSTRACT

The vibrational stability of detailed models of δ Cephei stars is studied by numerical integration of the linearized non-adiabatic pulsation equations. In contrast to a previous investigation, improvements in the method of integration allow the non-adiabatic calculations to be carried from the surface layers deep into the star. The periods are also determined from the models. It is found that both the period and the stability coefficient can be evaluated to high accuracy on the basis of the outer half (in mass) of the star. The effect of convection on the structure of the equilibrium models is included; the interaction of convection with the pulsations is neglected. Boundary conditions are discussed in detail in an appendix. A series of fifteen models of 7 M☉ lying along a portion of the evolutionary track calculated by Hofmeister, Kippenhahn, and Weigert has been investigated. The results confirm the existence of a region of linear instability, due largely to the destabilizing effect of second helium ionization, in a range of mean effective temperatures centered at about 5400° K. The instability is present for both the fundamental mode and the first overtone. In contrast to previous work, the hydrogen and first helium ionizations are found to contribute significantly to the destabilizing effect, especially for the overtones. The instability zone is wider in terms of effective temperature than is indicated by observations, and the temperatures of the most unstable models appear to be several hundred degrees lower than the observed temperatures of δ Cephei stars. The results are consistent with those of our previous work and of Cox. Possible consequences of the neglect of non-linear effects are discussed in a general way. The importance of the investigation of Cepheid pulsation as a check on the correctness of models for the evolution and structure of late-type stars in the helium-burning stages of evolution is pointed out.

I. INTRODUCTION

In this paper we discuss the non-adiabatic oscillations of rather detailed models of δ Cephei stars. We investigate the stability of infinitesimal radial pulsations of spherical stellar models by solving the fully non-adiabatic linearized equations of motion. Our main purpose is to understand how the instability depends upon the properties, particularly the observable properties, of the stars. This includes the attempt to identify on theoretical grounds the classical Cepheid region in the Hertzsprung-Russell diagram. We have attempted here to improve the linear methods to the point that a quantitative comparison with observation is beginning to be possible. In addition, as Cepheid calculations are refined and extended, we may hope that they will provide an important check not only on our present ideas as to the causes of Cepheid instability but also on the correctness of theoretical models for the structure and evolution of late-type giant and supergiant stars.

The possibility that the seat of the pulsational instability might lie in the region of second ionization of helium was suggested by Zhevakin and explored by him in a number of papers (a summary of some of this work and references to the original papers are found in Zhevakin 1963). Zhevakin used models consisting of a small number of discrete zones. Cox (1960) constructed models based on the "Woltjer method" in first approximation, and also found a strong tendency toward instability caused by second helium ionization. In a later paper, Cox (1963; hereinafter cited as "C63") integrated numerically the full set of non-adiabatic pulsation equations, as did the present authors (Baker

* Now at Department of Astronomy, Columbia University, New York.

† Now at Universitäts-Sternwarte, Göttingen.

and Kippenhahn 1962; hereinafter cited as "Paper I"). Although Cox used rather rough models, neglecting hydrogen and first helium ionization and taking very simple boundary conditions, he did consider carefully the structure of the second helium zone. He examined several different sequences of models and found regions of instability in the H-R diagram due to second helium ionization. Cox was able to conclude that this effect can account for the instability of the δ Cephei and RR Lyrae stars, and possibly also that of the W Virginis and δ Scuti variables. In Paper I we constructed models that did include the hydrogen and first helium ionization zones. On the basis of a very limited number of models, we also found pulsational instability due to second helium ionization in the δ Cephei region of the H-R diagram.

The present paper represents an extension of our previous work (Paper I). There are a number of major improvements, principally in technique. As in Paper I, the study is based on a series of equilibrium models (§ II). Previously the properties of these models were based on values inferred from observations; in the present work an evolutionary series of models for a star of 7 $M_\odot$ obtained by Hofmeister, Kippenhahn, and Weigert (1964a, b, c; referred to hereinafter as "HKW I," "HKW II," and "HKW III") was used. In contrast to Paper I, convection is now taken into account in the equilibrium models. The linearization of the equations is carried out in the usual way (§ III). In the absence of a satisfactory time-dependent theory of convection, we have made the *Ansatz* that the fraction of the energy flux which, in the equilibrium model, is carried by convection does not interact in any way with the pulsations. The boundary conditions are slightly different from those used in Paper I (§ III and Appendix). In that paper we also used periods based on observations; in the present work the proper periods have been calculated accurately from the models themselves (§ IV). The solution of the non-adiabatic equations (§ V) proceeds basically as before; however, a major improvement in the method of integration allows us to carry the integration from the surface as deep into the star as desired. In Paper I we were unable to use more than a few per cent of the star's mass, due to numerical difficulties; we are now using the outer half of the star's mass. It was found that this is more than enough to determine both the period and the stability coefficient to the desired accuracy. The stability coefficient is evaluated as in Paper I. The new techniques and the use of a much faster computer have enabled us to investigate both fundamental and overtone pulsations of a series of fifteen models along the evolutionary track. The results are presented in § VI. In § VII the results are discussed and compared with those of Cox (1963) and of Paper I, and some of the difficulties of the present approach are examined.

A preliminary report of this work at an earlier stage was given by Baker (1963a). An extensive application of the techniques described in this paper has been made to a number of series of models, in which parameters such as mass, mixing length, and composition are varied. These calculations will be reported in a later paper in this series.

II. THE EQUILIBRIUM MODELS

As in Paper I equilibrium models are constructed by integrating numerically the time-independent equations in the outer layers of a star ("envelope"). In all cases it is assumed that the chemical composition throughout the envelope is constant and that no production of either nuclear or gravitational energy occurs (L_r = const.).

The envelope consists of an *atmosphere* and a *subphotospheric region*. In the atmosphere only the equation of hydrostatic equilibrium is integrated, the temperature being determined from an assumed temperature–optical-depth relation. In the subphotospheric layers an energy-transport equation is also included in the integration. The machine program now used for the equilibrium models differs in some respects from that described in Paper I. The present version of the program has also been used for other purposes and is described in detail by Baker (1963b) and, with slight variations, in HKW I. Therefore, we give here only a general outline of the essential parts of the program.

In the atmosphere we have used the temperature–optical-depth relation for a gray atmosphere in Eddington approximation. The use of this formula rather than the non-gray formula of Paper I results in values for the photospheric pressure that agree better with those obtained from integration of model atmospheres for A stars (Osawa 1956). One expects the non-gray effects to be still less important in cooler supergiant atmospheres such as those of Cepheids. In the hydrostatic equation (2) of Paper I, we have now included the reduction of the effective gravity due to radiation (Unsöld 1955):

$$g_{\text{eff}} = g - \frac{\kappa \sigma T_e^4}{c}. \tag{1}$$

In each case the atmosphere integration is carried to optical depth $\tau = \frac{2}{3}$.

All the models discussed in this paper are based on the extreme Population I mixture ($X = 0.602$, $Y = 0.354$, $Z = 0.044$) used in the stellar evolution calculations of HKW II (the complete opacity table is reproduced in Table 1 of that paper). Line effects were not included. The entire opacity table (log κ as function of log ρ and log T) was stored in the machine. Values of log κ at the desired points were obtained by linear interpolation as described in Paper I.

Since the opacity table is now stored in terms of log ρ and log T instead of log P_g and log T, it is necessary to solve the ionization equations in the atmosphere as well as in the subphotospheric layers. The ionization calculation is carried out just as before, except that we now use an iteration method to solve simultaneously the Saha equations for the degrees of ionization of H, He, and He$^+$ (cf. Paper I, p. 122 n.).

The integration below the photosphere proceeds by solving the basic equations:

$$\frac{d \ln r}{d \ln P} = -\frac{rP}{G \rho M_r}, \tag{2}$$

$$\frac{d \ln M_r}{d \ln P} = -\frac{4\pi r^4 P}{GM_r^2}, \tag{3}$$

$$\frac{d \ln T}{d \ln P} = \begin{cases} \nabla_{\text{rad}} = \left(\frac{3}{16\pi a cG}\right) \frac{\kappa LP}{M_r T^4}, & (\nabla_{\text{rad}} < \nabla_{\text{ad}}) \\ \nabla_{\text{conv}}, & (\nabla_{\text{rad}} \geq \nabla_{\text{ad}}), \end{cases} \tag{4}$$

with $L = \text{const}$. When convection is present the temperature gradient ∇_{conv} in equation (4) is calculated with the mixing-length theory as described in HKW I (eqs. [6]–[20]). The mixing length l is described by the ratio l/H_p, where H_p is the local pressure scale height. In this paper we have used $l/H_p = 1.5$.

The auxiliary quantities: c_P, ∇_{ad}, $(\partial \ln \mu / \partial \ln T)_P$, $(\partial \ln \mu / \partial \ln P)_T$,

$$a = \left(\frac{\partial \ln \rho}{\partial \ln P}\right)_T, \qquad \delta = \left(\frac{\partial \ln \rho}{\partial \ln T}\right)_P, \tag{5}$$

are calculated as before. At each integration point the quantities $(\partial \ln \kappa / \partial \ln \rho)_T$ and $(\partial \ln \kappa / \partial \ln T)_\rho$ were obtained by numerical differentiation in the opacity table. From these the quantities

$$\kappa_P = \left(\frac{\partial \ln \kappa}{\partial \ln P}\right)_T = a \left(\frac{\partial \ln \kappa}{\partial \ln \rho}\right)_T, \tag{6}$$

$$\kappa_T = \left(\frac{\partial \ln \kappa}{\partial \ln T}\right)_P = \left(\frac{\partial \ln \kappa}{\partial \ln T}\right)_\rho - \delta \left(\frac{\partial \ln \kappa}{\partial \ln \rho}\right)_T, \tag{7}$$

needed for the pulsation equations are calculated.

The integration of the equilibrium models is carried from the surface to a point where $M_r = 0.5\ M$. As we shall discuss in detail in §§ IV and V, it proved desirable to carry the integration this deep in order to determine the pulsation period accurately. This also assures that all parts of the star that can contribute non-adiabatic effects to the pulsation are included.

From the evolutionary models of HKW II and III we know that it is justified to assume that the initial composition has remained unchanged in the outer half of the star's mass. These calculations also justify the assumption $L_r = $ const.; even in the most rapid evolutionary evolutionary crossings of the Cepheid strip, the change in L, due to secular contraction or expansion is very small for $M_r \geq 0.5\ M$.

In the previous paper it was necessary to use semi-empirical masses since evolutionary models for Cepheids did not exist. In the present paper, however, we have based our equilibrium models on the evolutionary track of HKW II and III, which is reproduced in Figure 1. The evolutionary track of a model of 7.0 $M_\odot$ crosses the region of the δ Cephei stars five times. The present calculations follow the second crossing since this is the slowest one; the models lie in that part of the evolutionary track which is indicated by the heavy part of the curve in Figure 1.
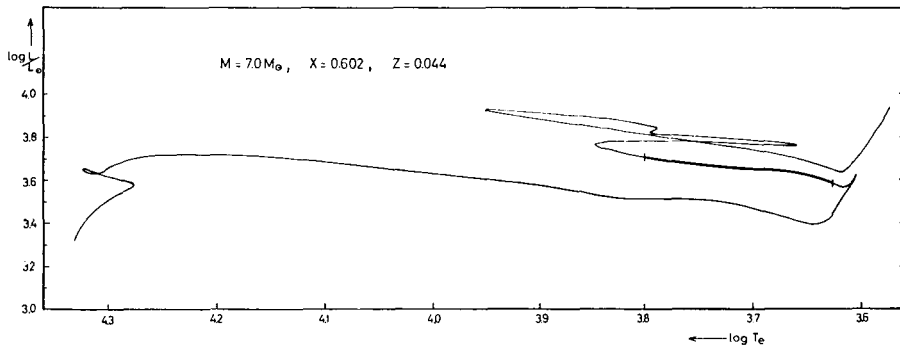

Fig. 1.—Evolutionary track for a star of 7 $M_\odot$, according to HKW III. The portion of the track studied in this paper is indicated by the heavy line.

In Table 1 are listed some of the properties of the models which were studied. Several of the models correspond exactly to evolutionary models obtained by HKW III. They are as follows: No. 1 = HKW 135, No. 7 = HKW 137, No. 9 = HKW 138. The parameters of the other models were obtained by interpolation and extrapolation from these. The second and third columns indicate the values taken for luminosity and effective temperature. The fourth column gives the photospheric pressure, and the next three columns indicate the approximate center of the ionization zones (in terms of log P_0). The eighth column lists the values of log P_0 at the top and bottom of the convection zones. Models 1–4 each have a single convection zone that includes all three ionization zones. Model 5 has two convection zones, one in the region of hydrogen and first helium ionization, another in the second helium ionization zone. Models 6–15 have relatively thin and ineffective convection zones that do not include the region of second helium ionization.

III. THE LINEAR OSCILLATIONS

We begin with the basic time-dependent equations for a spherically symmetric star. These are discussed in detail in § 4a of Paper I. The linearization of these equations proceeds in the usual way. We again introduce the non-dimensional variables x, p, t, and l, defined as

$$r = r_0(1 + x e^{i\omega\vartheta}), \quad P = P_0(1 + p e^{i\omega\vartheta}), \quad T = T_0(1 + t e^{i\omega\vartheta}), \quad L_r = L_0(1 + l e^{i\omega\vartheta}), \quad (8)$$

where r_0, P_0, T_0, and L_0 are solutions of the equilibrium equations and ϑ is the time variable. The linearized equations are then

$$\frac{dx}{d \ln P_0} = \frac{P_0 r_0}{GM_r \rho_0}(3x + ap - \delta t), \tag{9}$$

$$\frac{dp}{d \ln P_0} = -p - \left(4 + \frac{4\pi r_0^3 \bar{\rho}}{M_r}\sigma^2\right)x, \tag{10}$$

$$\frac{dt}{d \ln P_0} = \nabla_{\rm rad}[l - 4x + \kappa_P p + (\kappa_T - 4)t], \tag{11}$$

$$\frac{dl}{d \ln P_0} = i\sigma \frac{4\pi P_0^2 r_0^4 \delta}{L_0 M_r \rho_0} \sqrt{\left(\frac{4\pi\bar{\rho}}{G}\right)} \left(\frac{1}{\nabla_{\rm ad}}t - p\right). \tag{12}$$

TABLE 1

PROPERTIES OF THE MODELS

MODEL	LOG $L/L_\odot$	LOG T_e	LOG P_0					Π_0 (days)	Π_1 (days)	Q_0 (days)	Q_1 (days)
			Photo-sphere	H I Zone	He I Zone	He II Zone	Convection Zone(s)				
1.....	3.587	3.628	3.46	4.07	4.99	6.13	3.80–8.44	25.8	14.4	0.0553	0.0294
2.....	3.603	3.650	3.43	3.98	4.64	5.52	3.76–6.95	20.5	12.7	.0496	.0303
3.....	3.617	3.669	3.41	3.91	4.42	5.09	3.73–5.78	17.3	11.5	.0468	.0309
4.....	3.627	3.680	3.41	3.87	4.30	4.87	3.71–5.20	15.9	10.8	.0454	.0310
5.....	3.636	3.690	3.40	3.84	4.22	4.78	3.69–4.41 4.69–4.94	14.7	10.2	.0444	.0309
6.....	3.647	3.710	3.41	3.77	4.07	4.70	3.66–4.16	12.7	9.04	.0432	.0307
7.....	3.663	3.726	3.41	3.72	3.96	4.68	3.62–4.00	11.5	8.26	.0423	.0304
8.....	3.671	3.740	3.41	3.67	3.86	4.63	3.59–3.89	10.4	7.52	.0417	.0302
9.....	3.676	3.750	3.40	3.64	3.80	4.63	3.56–3.82	9.71	7.07	.0412	.0300
10.....	3.678	3.760	3.39	3.60	3.74	4.63	3.53–3.75	8.96	6.55	.0408	.0298
11.....	3.681	3.770	3.37	3.55	3.68	4.63	3.50–3.68	8.32	6.12	.0403	.0297
12.....	3.684	3.780	3.35	3.51	3.62	4.63	3.46–3.60	7.72	5.70	.0399	.0295
13.....	3.687	3.790	3.32	3.46	3.56	4.63	3.42–3.54	7.18	5.31	.0396	.0293
14.....	3.688	3.800	3.28	3.41	3.50	4.63	3.38–3.47	6.67	4.95	.0392	.0291
15.....	3.691	3.810	3.23	3.35	3.44	4.63	3.33–3.40	6.19	4.60	0.0389	0.0289

The (Lagrangian) independent variable is the logarithm of the equilibrium pressure belonging to a given mass shell. We have also introduced the dimensionless frequency

$$\sigma = \omega/\sqrt{(4\pi G\bar{\rho})}, \tag{13}$$

where $\bar{\rho}$ is the mean density of the star.

Equation (11) is valid only in those regions where all of the energy is transported by radiation. In the convection zones there arises the problem of dealing with the time variation of the convective energy flux. The mixing-length theory used for the equilibrium models is a steady-state theory; a simple linearization of these equations would be valid only if the convective time scale were small compared with the pulsation period. Simple estimates indicate that this will not be the case everywhere in the outer convection zone of a star. A physically correct treatment of the pulsations of the convective regions would require the use of a time-dependent theory of convection (this problem has been studied by Christy 1962). We therefore have made the assumption that the

convective part of the energy flux is completely unaffected by the pulsation. Thus we separate the flux into a radiative part plus a convective part:

$$L_r = L_r{}^R + L_r{}^C , \tag{14}$$

and we assume that $L_r{}^C$ is at all times equal to $L_{r0}{}^C$, the equilibrium value. If we define l^R by

$$L_r{}^R = L_{r0}{}^R (1 + l^R e^{i\omega \vartheta}), \tag{15}$$

then l^R and l are related by

$$l^R = (L_0/L_{r0}{}^R)l . \tag{16}$$

The equation for the radiative flux,

$$\frac{dT}{d \ln P} = \frac{3 \kappa P L_r{}^R}{16 \pi a \, c G M_r T^3} \tag{17}$$

has the linearized form

$$\frac{dt}{d \ln P_0} = \nabla_0 \left[\frac{L_0}{L_{r0}{}^R} l - 4x + \kappa_P p + (\kappa_T - 4) t \right], \tag{18}$$

where

$$\nabla_0 = \frac{d \ln T_0}{d \ln P_0}. \tag{19}$$

Thus we replace equation (11) by equation (18), which reduces to equation (11) in radiative regions.

The pulsation equations (9), (10), (12), and (18) apply to the subphotospheric region of the equilibrium models. The properties of the atmospheric pulsations are not considered here and appear only in the boundary conditions that are applied to the pulsation equations at the photosphere.

The thermal boundary condition at the photosphere ($\tau = \frac{2}{3}$) is

$$l = 3x + (4 - \tfrac{1}{2}\kappa_T)t - \tfrac{1}{2}\kappa_P p . \tag{20}$$

This condition differs slightly from that used in Paper I and also from that derived in the more detailed considerations of Unno (1964) (the boundary conditions are discussed in detail in the Appendix). The mechanical boundary condition is that appropriate to isothermal or adiabatic oscillations of an isothermal atmosphere,

$$p = -(3\sigma^2 + 4)x , \tag{21}$$

which is equivalent to

$$\frac{dp}{d \ln P_0} = 0 . \tag{22}$$

This condition is derived in the Appendix. The same condition was derived in a different way in Paper I but differs somewhat from the condition used for most of the models of that paper. It also agrees with that used in C63.

If we were using a complete stellar model, the inner boundary condition would be the requirement of regularity at the center. Since, however, our equilibrium model does not extend to the center, we must apply some condition at the inner boundary of the envelope. Therefore we require that, at the inner boundary, the envelope solution must fit exactly to the adiabatic oscillation of the interior. Thus we require

$$t = \nabla_{\mathrm{ad}} p \tag{23}$$

at the inner boundary of the envelope. Since this point is so deep that the factor

$$\frac{4\pi P_0{}^2 r_0{}^4 \delta}{L_0 M_r \rho_0} \sqrt{\left(\frac{4\pi \bar{\rho}}{G} \right)}$$

in equation (12) is very large compared with unity, any solution that is regular at the center will also fulfil condition (23) to a high degree of accuracy.

In general the eigenvalue σ is complex and we are free in addition to specify a complex normalizing factor. If we omit the interior and instead apply condition (23) at the inner boundary of the envelope, then the system of equations (9)–(12) with conditions (20), (22), and (23) can be integrated for any given value of σ. Since the eigenvalue is a property of the entire star, one might expect it to be impossible to determine σ on the basis of a model of the outer layers alone. In fact it turns out that both the real part of σ, which determines the period, and the imaginary part of σ, which determines the damping coefficient, may be obtained to a high degree of accuracy by consideration of the envelope alone.

In order to determine both parts of σ, which is the object of this investigation, the missing interior must be replaced by suitable additional conditions on the envelope solution. The way in which this is done will be described in the next two sections.

IV. DETERMINATION OF THE PERIODS

In Paper I we chose the periods on the basis of a semi-empirical period–mean-density relation. This had the consequence that some of the periods chosen were quite different from the actual fundamental periods appropriate to the models. Indeed, some of our fundamental solutions had overtone characteristics, as was pointed out by Ledoux (private communication). In the present paper we determine the periods purely theoretically from the models themselves.

If we apply the adiabatic condition (23) at each point, then equations (9) and (10) together with the boundary condition (21) can be solved for any given value of σ (adiabatic approximation). The solutions p and x will satisfy regularity conditions at the center only for a certain set of (real) eigenvalues σ_i ($i = 0, 1, 2, \ldots$). It turns out to be possible to determine the first two eigenvalues to a sufficient degree of accuracy on the basis of the envelope model alone. This is especially true for the fundamental mode of stars with high central condensation (cf. Epstein 1950).

The eigenvalue is determined by requiring that the behavior of the functions in the envelope be consistent with the regularity conditions at the center. For example, the fundamental oscillation with frequency σ_0 which fulfils the regularity condition will have no zeros in either x or its (space) derivative, except at the center. Therefore if a solution using a trial value of σ_0 has a zero in x or in $dx/d \ln P_0$ in the envelope, its continuation in the interior could never satisfy the regularity condition at $M_r = 0$. The direction in which x tends to diverge tells us how σ must be changed.

The search for the eigenvalue σ_0 proceeds as follows: A (real) trial value for σ_0 is chosen and the second-order set of pulsation equations for the adiabatic approximation, with the boundary condition (21), is integrated from the surface inward. If the function x changes sign, one knows that the trial frequency is greater than σ_0. If x does not change sign, and its derivative $dx/d \ln P_0$ does change sign, it is an indication that the trial value is too low. The procedure is illustrated in Figure 2 for a typical model of our series. In this case it is seen that the difference between the upper and lower limits to σ is less than 0.65 per cent. This method works particularly well for stars in the Cepheid region; both hotter and cooler stars of similar mass and luminosity are less centrally condensed, and for them a larger fraction of the mass would have to be used to obtain the same accuracy.

The method may be extended to obtain the overtone frequencies σ_i by requiring that the ith overtone have exactly i nodes both in the function x and in its derivative. The accuracy becomes somewhat poorer for higher overtones. Nonetheless, we are able to determine the periods to an accuracy of ± 0.4 per cent for the fundamental mode and ± 0.6 per cent for the first overtone for all the models of our series except models 1 and 2. These cool models have very deep convection zones and consequently are not very condensed.

In model 1, for example, the fundamental period could be determined to only about ± 20 per cent. The period and the pulsation constant

$$Q = \Pi \sqrt{(\bar{\rho}/\bar{\rho}_{\odot})} \tag{24}$$

of the fundamental mode and first overtone for all models of the series are given in the last four columns of Table 1.

Since complete stellar models are available for some of the equilibrium models in the present investigation, it would be possible to use them to calculate the periods to very high accuracy. Such calculations have been carried out by Temesvary (1964); the periods obtained confirm those computed by the method described above. In general our method is more than sufficiently accurate for the present purpose.
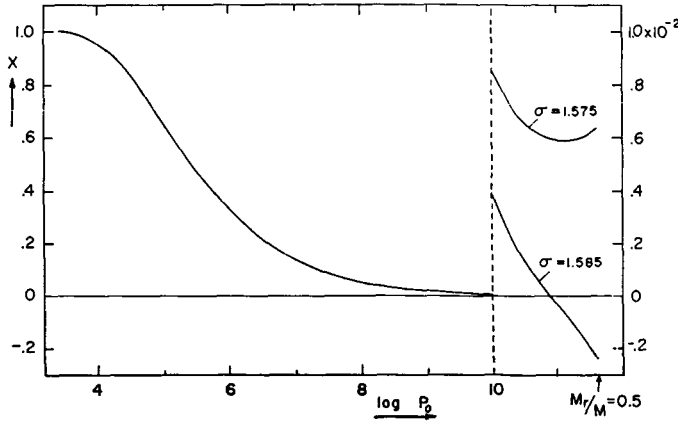
FIG. 2.—Method used to determine the period. The function x is plotted for the adiabatic pulsations of model 7 of our series. The scale is increased by a factor of 100 for $\log P_0 > 10.0$ in order to show the different behavior of the function for two slightly different values of σ. The arrow indicates the value of $\log P_0$ corresponding to $M_r = 0.5\ M$.

The inclusion of non-adiabatic effects would change the periods only slightly. This can be expressed in terms of the non-adiabatic parameter η, defined by equation (29), which is approximately the ratio of the period to the damping time of the star. The relative change in frequency due to non-adiabatic effects will be of order η^2 (cf. Ledoux 1963; Baker 1965). In most of our models $|\eta|$ is of order 10^{-4}, and the maximum value found is approximately 3×10^{-3}. Hence non-adiabatic effects will change the period by no more than one part in 10^5, and we may safely use the adiabatic periods.

V. THE NON-ADIABATIC MODELS

When the eigenfrequency has been found from the adiabatic equations the solution may be extended to obtain the *quasi-adiabatic approximation* to the non-adiabatic system. This is done in the following way: from the adiabatic solution we know the value of p and x at each point. Then we find t from equation (23) at each point and its derivative from

$$\frac{dt}{d \ln P_0} = \nabla_{\rm ad} \frac{dp}{d \ln P_0} + p \frac{d\nabla_{\rm ad}}{d \ln P_0}, \tag{25}$$

with

$$\frac{d\nabla_{\rm ad}}{d \ln P} = \left(\frac{\partial \nabla_{\rm ad}}{\partial \ln P}\right)_T + \left(\frac{\partial \nabla_{\rm ad}}{\partial \ln T}\right)_P \nabla. \tag{26}$$

Then l can be obtained from equation (18). The set of functions x, p, t, and l so obtained is used as the first trial solution in our iterative method of solving the fully non-adiabatic pulsation equations.

The next step is to solve the set of non-adiabatic linear equations (9)–(12), using the frequency σ found in the adiabatic calculation. Here the method of integration plays a significant role in the accuracy of the results. Since we are dealing with a linear system, the most straightforward method is to construct trial solutions which may then be combined to satisfy the boundary conditions. This was the method used in Paper I; as we pointed out there, it has important disadvantages when the integration is carried into the nearly adiabatic interior. When this method was used, we were forced to terminate the integration at a rather small value of log P_0, and it was necessary to estimate the damping due to the interior. In order to overcome this problem we attempted to construct a complete solution for the outer 50 per cent of the star's mass by fitting the non-adiabatic solution in the outer part of the envelope to the quasi-adiabatic solution in the deeper layers of the envelope. This method was only moderately satisfactory and required use of double-precision calculations.

A completely satisfactory method was found only by going to an iterative method of solution. It was found that a relaxation method, similar to that which has proved most satisfactory for numerical integration of the non-linear equations of stellar structure (Henyey, Forbes, and Gould 1964), also can be applied very successfully to our linear equations. With this method it is possible to integrate the full non-adiabatic equations as deep as desired, well into the adiabatic interior regions. These solutions then have a smooth transition from the non-adiabatic character outside to the adiabatic character inside. It is no longer necessary to estimate the interior damping.

The procedure described above uses the value of σ found from the adiabatic calculation. This quantity is real and is a good approximation to the real part σ_R of σ in the general case. We wish, however, to determine the imaginary part σ_I of σ. Since this must be done on the basis of the envelope model alone, an additional condition is required. Physically this condition is that energy must be conserved in the star as a whole. Instead of actually solving for σ_I, we use the approximate method of the energy integral described in Appendix C of Paper I. The non-adiabatic equations are integrated using the real value of σ from the adiabatic model. Then the energy integral

$$W = 4\pi^2 P_0 r_0{}^3 Im(p^*x) \tag{27}$$

is evaluated at the inner boundary of the envelope. Call this value W_i. Since the interior part of the envelope is highly adiabatic, the value of W_i is independent of the point chosen for the inner boundary of the envelope, so long as this is sufficiently deep (see Fig. 4). To get an estimate of σ_I we normalize W_i with respect to the total pulsational energy of the star:

$$W_p = \frac{\sigma_R{}^2}{2} \int_0^M |x|^2 r_0{}^2 dM_r . \tag{28}$$

Since the integrand in equation (28) is very small in the interior compared with its value in the outer layers, W_p may be very accurately approximated by carrying the integration over the envelope alone. We then define the stability coefficient:

$$\eta = W_i/W_p , \tag{29}$$

which is approximately equal to the ratio $-\sigma_I/\sigma_R$.

VI. THE RESULTS

For each of the models listed in Table 1 an equilibrium model was constructed by integrating equations (2)–(4) from the surface to the level $M_r = 0.5\ M$. Then the periods

Π_0 and Π_1 for the fundamental mode and first overtone of each model were obtained from the adiabatic equations by the method described in § IV. With these periods the non-adiabatic equations were then integrated numerically.

The results of this integration in a typical case are shown in Figure 3. Both real and imaginary parts of the functions x, p, t, and l are plotted as functions of log P_0. (For numerical convenience, log P_0 was used as the independent variable in the calculations. In order to show more detail, the functions are plotted only as far as log $P_0 = 9.0$; in
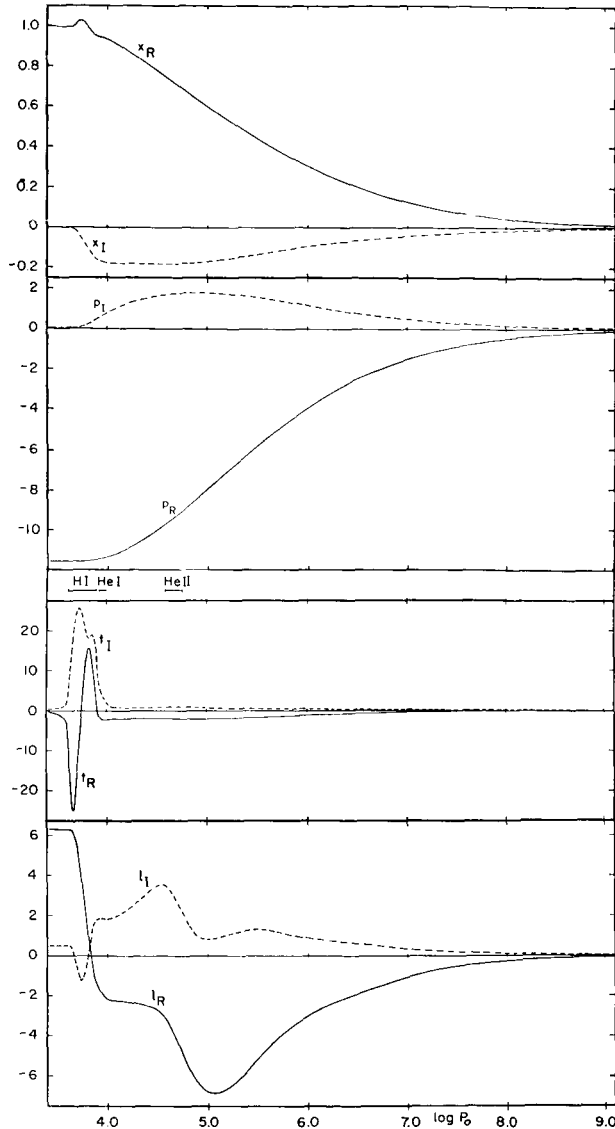
FIG. 3.—Real and imaginary parts of the fluctuations for model 7. The hydrogen, first helium, and second helium ionization zones are indicated.

general the calculations were carried to a value of log P_0 between 11.0 and 12.0, in order to reach the desired depth in mass.)

The normalization constant is chosen so that $x_R = +1.0$, $x_I = 0$, at the photosphere. The hydrogen, first helium, and second helium ionization zones are indicated. (For this purpose we have defined the "ionization zones" to be those regions where $\nabla_{ad} < 0.2$ due to ionization.) The non-adiabatic effects in the outer layers are reflected in the strong variation of the thermal quantities t and l, while the mechanical quantities x and p remain quite smooth. Figure 3, which refers to the fundamental mode of model 7 of our series, may be compared with similar figures in Paper I. The general run of the variables is similar; the chief differences are due to the change in the boundary conditions.
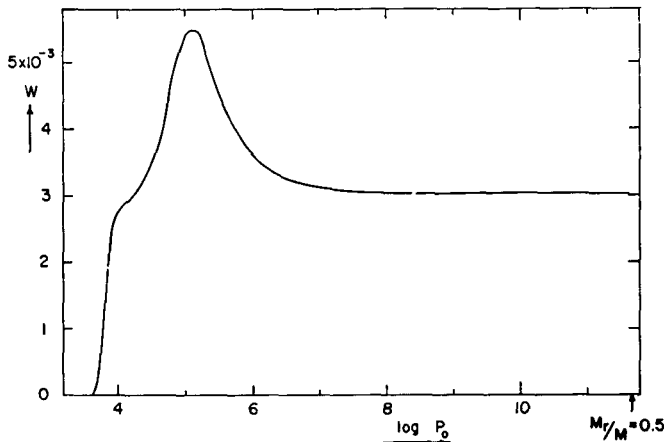
FIG. 4.—The w-integral for model 7. The arrow indicates the value of log P_0 corresponding to $M_r/M = 0.50$. The curve becomes horizontal long before this point is reached, indicating that the inner boundary of the envelope lies deep inside the adiabatic interior.

For each model the energy integral W as defined by equation (27) was calculated at every point, and W_p was obtained by integrating the pulsational energy through the entire envelope. Then the "normalized energy integral,"

$$w = W/W_p \tag{30}$$

can be computed at each point. The behavior of w shows whether a particular region of the star produces positive or negative damping. If $dw/d \log P_0$ is positive in a particular region, it means that this region contributes a destabilizing effect; conversely, a negative value of the derivative indicates a layer that contributes damping. In the adiabatic interior the derivative goes to zero and, from the definition (30), η is equal to the value of w at the inner boundary of the envelope.

In Figure 4 we have plotted the function w for the fundamental mode of model 7 of our series (this is the same model as in Fig. 3; it corresponds to model 137 of HKW III). From this figure one sees that, in contrast to Paper I, we have here carried the calculations deep enough into the star's interior that w becomes essentially constant. Therefore the central value of w, which determines the total amount of damping or excitation of the star, is known without our having to carry the integration into the central region or to estimate the contribution of the interior. In order to give an idea of the depth of the envelope in terms of log P_0, the point at which $M_r = 0.5\,M$ has been indicated.

In Figure 5, w is plotted for the fundamental mode of five models of our series.

Figure 5, *a–e*, correspond to models 15, 12, 7, 4, and 1, respectively, of our series, going from the model having the highest effective temperature to that having the lowest. Since the value of w at the right-hand side of each figure is equal to η for the corresponding model, one can see that model 15 is stable, the others being unstable with maximum instability occurring somewhere near model 7.

Figure 6 shows the behavior of w for the first overtone of model 7. This may be compared with the fundamental for the same model, shown in Figure 5, *c*. The overtone pulsation is somewhat more unstable. The contribution to w from the hydrogen–first helium ionization zone is much greater relative to that from the second helium ionization
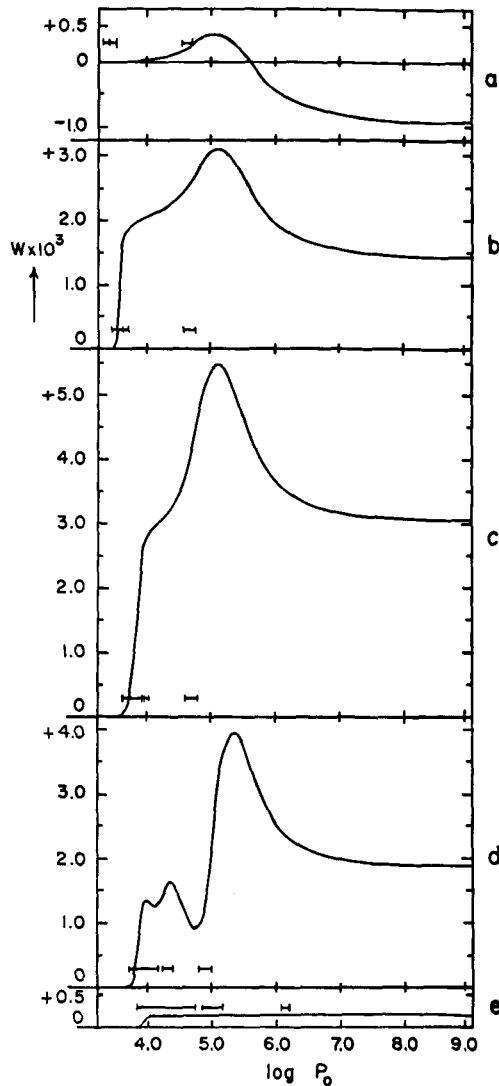
Fig. 5.—The w-integrals for models 15(*a*), 12(*b*), 7(*c*), 4(*d*), and 1(*e*) of the series. Ionization zones for hydrogen, first helium, and second helium are indicated.

zone. This is due chiefly to the relatively greater amplitude of the fluctuations in the outer layers for the overtone pulsations. (The amplitude of x, e.g., falls more steeply going inward from the surface, and for the model of Figure 6 the node is at log $P_0 \approx 5.9$. The amplitude is very small interior to the node.)

The final result of the calculation for each model is then the stability coefficient η. In Figures 7 and 8 we have plotted, for fundamental mode and first overtone, respectively, the value of η along the part of the evolutionary track here investigated, using log T_e as abscissa. Both modes have a maximum instability near models 7 or 8 ($T_e \approx 5400°$). The horizontal arrows in Figures 7 and 8 show the observed fluctuation amplitude in T_e of the Cepheid η Aql, according to Oke (1961). Although the comparison with η Aql is not exact
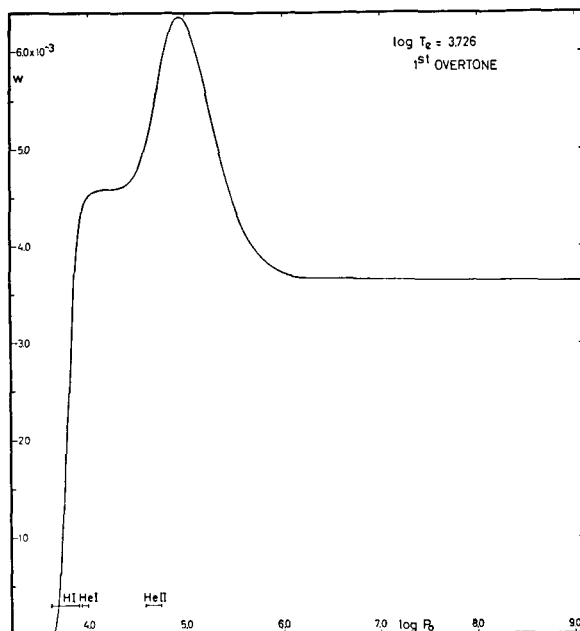

FIG. 6.—The w-integral for the first overtone of model 7

(the models here investigated are approximately $0^m.4$ brighter than η Aql in mean bolometric magnitude), it is apparent that the mean effective temperature of the most unstable models is several hundred degrees lower than that of η Aql. The width of the instability zone in terms of log T_e is about twice as great as the observed temperature fluctuation of η Aql.

Some features of the way in which the contributions of various layers to the damping or excitation depend upon effective temperature may be seen from an inspection of Figure 5. In the first model (Fig. 5, a), there is a destabilizing region due to second helium ionization in the neighborhood of log $P_0 = 4.6$. This effect, however, is more than canceled by the damping in the deeper-lying non-adiabatic zone where helium is completely ionized. The hydrogen and first helium ionizations occur in the outer layers and have a negligible effect. In the slightly cooler model of Figure 5, b, all three ionization zones have moved deeper and they are all making a greater contribution. The damping in the deeper-lying part of the non-adiabatic zone is decreased because the second helium ionization occurs deeper. The initial rise in w at the left is due to both hydrogen

and first helium ionization. In the next cooler model (Fig. 5, c), all of these effects have increased. In the still cooler model of Figure 5, d, the destabilization due to second helium ionization has become still larger. The contributions of the hydrogen and first helium ionization zones, however, have decreased. The reason is that these zones are now becoming convective; according to our assumptions (§ III), that portion of the energy flux which is carried by convection cannot contribute to damping or excitation. The existence of convection also means that the ionization zones become more extended, covering a larger range in log P_0. For this reason it is possible to resolve the separate effects of hydrogen and first helium ionization in Figure 5, d. In the very cool model of Figure 5, e, one can see what happens when the entire inner envelope, including the
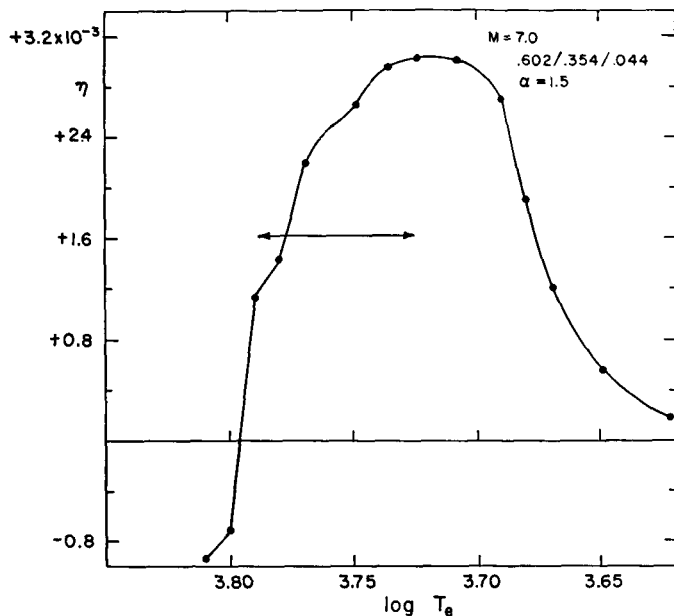

FIG. 7.—The stability coefficient η as a function of log T_e for the fundamental mode of all models of the series.

second helium ionization zone, becomes largely convective. Whether ionization occurs or not, no region of the envelope makes much contribution to damping or excitation; only that small portion of the flux which is radiative can have any effect. At these low surface temperatures a fully convective envelope is approached; such an envelope must, in our treatment, have neutral stability.

In Figure 9 is plotted the phase shift ϕ between l and x as a function of depth, again for model 7. The sign of ϕ is such that a value $0 < \phi < 180°$ means that maximum l occurs before maximum x. In the interior regions $\phi \approx 180°$, in agreement with the quasi-adiabatic approximation, which is valid there. Going toward the surface, ϕ increases slightly in the region of positive damping interior to the second helium zone, then decreases where the damping is negative due to second helium ionization. Another slight increase in ϕ outside the second helium zone is followed by a sudden drop in the first helium and hydrogen ionization zones. The resulting value of ϕ at the surface is nearly zero.

It may be noted that the sense of the change in ϕ is related to the sense of the damping

in any particular region: positive damping corresponds to $d\phi/d \ln P_0 < 0$ and vice versa. On the other hand, the magnitude of the phase shift does *not* reflect the magnitude of the contribution of a layer to the positive or negative damping. For example, the second helium zone and the hydrogen–first helium zone each contribute about the same amount of excitation in model 7, but the phase shift in the latter zone is much greater. The resulting phase shift at the surface appears to depend less upon the total amount of negative damping than upon the region of the star in which this effect occurs.
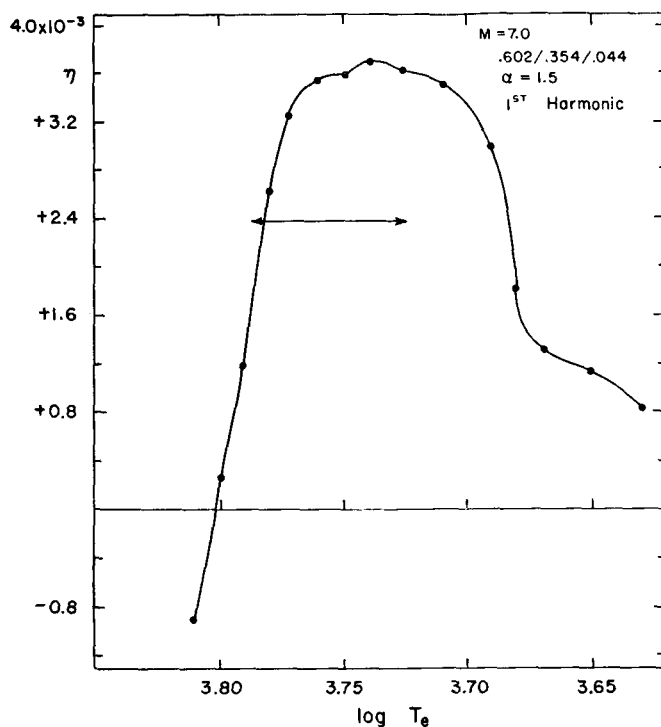
Fig. 8.—The stability coefficient η as a function of $\log T_e$ for the first overtone of all models of the series.
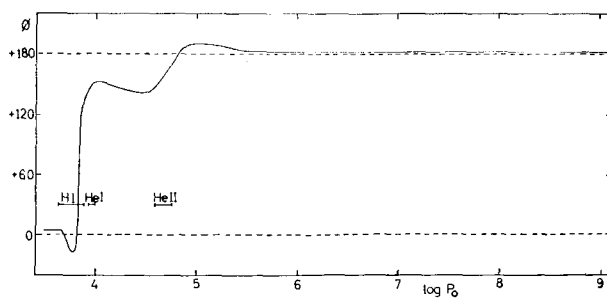

Fig. 9.—Phase shift between l and x as a function of depth for model 7. Ionization zones are indicated

VII. CONCLUSIONS AND DISCUSSIONS

Although the evolutionary calculations show that a star may pass through the Cepheid region several times during its history, we have here investigated only a single such crossing. This investigation has shown that a star becomes vibrationally unstable when it enters a region in which the surface temperature is about 5000°–6000° K. Hotter models are decidedly stable; for cooler models we can say that the instability mechanism investigated here cannot be effective. Stability calculations for a few models corresponding to the other crossings have also been made but are not discussed here in detail. These calculations show that a star of given mass becomes unstable in about the same range of effective temperatures each time it crosses the Cepheid strip. This is to be expected since the outer layers for all the crossings are nearly the same for a given effective temperature (cf. Fig. 1).

The luminosity of the star remains essentially constant during any single crossing of the Cepheid strip. However, since a star of a given mass may cross the strip several times, there will not be a unique mass-luminosity relation for Cepheids. The difference in luminosity from one crossing to another, although it is not very great, does have the consequence that we would not expect a unique period-luminosity relation to exist, even if the width of the instability strip in T_e were very small. From an observational viewpoint, however, the dispersion in the period-luminosity relation resulting from the non-unique mass-luminosity relation will be small compared with that due to the finite width of the strip.

The present results are in qualitative agreement with those of Paper I and with those of C63. In contrast to both of the above works we have calculated the periods from the models themselves (the pulsation constants agree quite well with those assumed in C63). A second difference is the freedom from the necessity of estimating the contribution of the interior to the damping. In Paper I we investigated only a few isolated models, while in C63 several series of models were studied, the models in each series having a given mass and luminosity, the radius being varied. In this sense the present paper is similar to C63, except that we can now follow an actual evolutionary sequence of models of given mass. (In practice the luminosity is nearly constant throughout the series.)

Our results confirm the conclusions in Paper I and in C63 that the second helium ionization zone plays an important role in producing linear pulsational instability in Cepheids. On the other hand, the hydrogen and first helium ionization zones now contribute as much or more to the excitation in some cases as does the second helium zone. This effect is not seen in the models of Paper I (C63 does not consider hydrogen and first helium ionization). The main reason for the difference is that the hydrogen and first helium zones are much more extended in the present models due to convection, which was neglected in Paper I. Thus for a model of given M, L, and T_e, the amount of mass in the ionization zones is considerably greater when convection is taken into account. To a lesser extent, the different boundary conditions also play a role. As was seen in comparing models I_6 and I_6' of Paper I, the nature of the pulsations, especially in the hydrogen ionization zone, is quite dependent upon the photospheric boundary condition.

The present calculations have shown that a region of pulsational instability exists for stars having effective temperatures near the observed temperatures of the classical Cepheids. The calculated periods near the point of greatest instability are nearly in agreement with observed periods.

On the other hand there are still a number of difficulties. The range of effective temperatures for which instability appears is considerably greater than the observed width of the Cepheid strip. Also, the maximum of the instability lies at an effective temperature several hundred degrees lower than the apparent center of the observed Cepheid

region.[1] Our calculations also indicate that the first overtone should be at least as strongly excited as the fundamental. This does not appear to be observed. Finally the calculations do not predict the observed phase shift of roughly 90° between the radius and luminosity fluctuations.

All of the above cases of failure to predict observational details may reflect the inherent limitations of the linear-stability analysis. Our treatment shows only that certain stars will be unstable against infinitesimal pulsations. The amplitude is determined by non-linear effects which set a limit to the growth of the pulsation. Two stars that have the same value of η may have quite different amplitudes. Therefore some stars that, according to the linear theory, are clearly unstable may pulsate with a very small amplitude and thus appear to the observer to be stable. The observed Cepheid strip hence might be expected to be thinner than the theoretical one.

The linear models may also be misleading when one compares the contributions of different layers of the star to the damping or excitation. In a full-amplitude pulsation the relative contributions may be quite different, because the non-linear effects may differ greatly from one region to another. From Figure 3, for example, we see that the amplitudes of all the functions, and particularly that of l, are much greater in the hydrogen ionization zone than in the second helium zone. Thus, as the amplitude increases with time, we may expect non-linear effects to become important first in the hydrogen zone. An additional effect is the fact that the hydrogen ionization "saturates" much sooner, due to the lower ionization potential. Hence, this zone may, at large amplitude, be driven so hard by the rest of the star that ionization is complete long before the maximum temperature is reached. In such models the linear calculations could greatly overestimate the destabilizing effect of the hydrogen zone.

If we were to discount the destabilizing effect of the hydrogen ionization zone in large-amplitude pulsations, many of our models, particularly those on the edges of the instability strip, would be more stable. The strip would be narrower, and its center would be shifted. It appears from preliminary calculations that this shift would be to the right, thus making the discrepancy with the observed effective temperatures greater. It would also have the effect of making the overtone pulsations much more stable, since the instability we have found for the overtones is caused almost entirely by the hydrogen and first helium ionization zones. Indeed, from a comparison of Figures 5, c, and 6 it can be seen that the overtone pulsation of model 7 would be stable if that part of the excitation due to hydrogen and first helium ionization were neglected. The fundamental mode would still be unstable, although less so.

From Figure 9 it is seen that the phase shift at the surface depends, in our calculation, very strongly on the complicated situation in the outer layers, particularly in the hydrogen ionization zone. Since the non-linear effects are apparently most important just in this zone, it is perhaps not surprising that the linear theory does not give satisfactory results for the phase shift.

The above problems, which are inherent to the linear theory, can probably be solved only by integrating the complete set of non-linear equations. Such calculations have been begun by Christy (1964) and by Cox and collaborators (Cox 1965); they should provide an important check on the linear theory.

The present treatment of convection, which ignores the interaction with the pulsations, cannot be considered satisfactory. Within the present framework, however, it is possible to indicate qualitatively what would happen if the assumed effectiveness of con-

---

[1] This was also found in C63 and was emphasized by Baker (1963a). It is not clear whether this discrepancy is serious or not. It may indicate that the structure of our equilibrium models needs to be changed slightly. Preliminary investigations (Baker 1963a and unpublished) indicate that the location of the instability strip may be sensitive to the assumptions made as to chemical composition and convection in the model envelope,

vection in the equilibrium models were changed. If it is assumed that the mixing-length theory with l/H_p equal to 1.5 greatly overestimates the convection, so that the energy flux in even the coolest models is carried almost wholly by radiation, the instability strip would extend to much lower effective temperatures. The instability would continue until the effective temperature is so low that even the hydrogen ionization takes place in the adiabatic interior. This would lead to a very considerable contradiction with the observed width of the Cepheid strip. If, on the other hand, the convection is more effective than we have assumed, the instability strip would move to the left and become narrower. This would appear to give better agreement with observation. In the models this effect could be produced by basing the calculations of the equilibrium models on a larger value of the mixing length. The effect reflects only the change in the stratification of the sub-photospheric layers as a consequence of convection. Some of these points will be discussed in detail in a later paper.

Because the properties of the pulsation do not depend upon the interior structure it would at first appear that the occurrence of the Cepheid phenomenon can give us little information about the evolutionary history of a star. An exception to this is the possibility of observing period changes. As the star's radius changes during its nearly horizontal passage through the Cepheid strip, the period will increase or decrease depending upon whether the effective temperature decreases or increases. Since the time scale for the change in effective temperature is controlled by the evolutionary changes in the most central region, the rate of change of period might be a very sensitive test of the correctness of presently accepted ideas about the helium-burning stages of stellar evolution. The sense of the period change shows whether the star is on a crossing from left to right or vice versa. The magnitude of the relative period changes for a star of 7.0 $M\odot$ is expected to be of the order of 0.01 per cent in 100 years, for the three slowest crossings (HKW III). Presently available observations do not appear to be in contradiction with the theoretically predicted period changes (Hofmeister *et al.* 1965). However, more observational material relating to period changes in Cepheids would be highly desirable.

On the other hand the pulsational properties are quite sensitive to the structure of the outer layers. Thus it may be conjectured that the period changes observed in some Population II Cepheids are somehow related to changes in the structure of the outer layers. Among other things the depth of the outer convection zone will affect the period. As the Cepheid calculations become more detailed and refined, it may be possible to infer information about the outer convection zone through a comparison of observed and calculated periods. Nor can we rule out the possibility that the structure of the convection zone may have a significant influence on the stability.

APPENDIX

THE SURFACE BOUNDARY CONDITIONS

The boundary conditions to be applied to the set of equations (9), (10), (12), and (18) at the photosphere should be obtained by a detailed consideration of the pulsations of the atmosphere. This has recently been done by Unno (1964). At the time our calculations were carried out, however, Unno's work was not available; therefore we have used boundary conditions derived from a very simple model of a pulsating atmosphere. Here we describe this simple model and compare the boundary conditions derived from it with those obtained by Unno. We also discuss some numerical tests that were carried out to see how the stability calculations are affected by the boundary conditions. Finally, we consider the effect of applying a running-wave boundary condition instead of the usual requirement of standing waves.

a) The Thermal Condition

The thermal boundary condition was obtained (cf. Paper I, p. 128) simply by linearizing the temperature–optical-depth relation:

$$T^4 = \tfrac{3}{4} \frac{L}{\pi a c r^2} (\tau + \tfrac{2}{3}) . \tag{A1}$$

Let d be the non-dimensional fluctuation in τ:

$$\tau = \tau_0 (1 + d \, e^{i\omega\vartheta}) . \tag{A2}$$

The linearized form of equation (A1) is then

$$4t = l - 2x + \left(\frac{\tau_0}{\tau_0 + \tfrac{2}{3}} \right) d . \tag{A3}$$

If we now write, as in Paper I,

$$d\tau = - \frac{\kappa}{4\pi r^2} \, dM_r \tag{A4}$$

and integrate this equation through the atmosphere, we obtain

$$\tau = \frac{\langle \kappa \rangle m}{4\pi r^2} , \tag{A5}$$

where m is the mass of the atmosphere. In performing the integration we have assumed r to be constant; $\langle \kappa \rangle$ is then a mean value for κ in the atmosphere, assumed to be weighted according to mass and so as to take into account the neglected variation of r. We then make the additional assumption that this mean value of κ will not differ greatly from the value of κ at the point where the condition is applied. Thus we set

$$\langle \kappa \rangle = \kappa \tag{A6}$$

in equation (A5). The linearized form of this equation is then

$$d = - 2x + \kappa_T t + \kappa_P p ; \tag{A7}$$

upon substituting this into equation (A3) we obtain the condition

$$l = 2 \left(1 + \frac{\tau_0}{\tau_0 + \tfrac{2}{3}} \right) x + \left(4 - \frac{\tau_0 \kappa_T}{\tau_0 + \tfrac{2}{3}} \right) t - \left(\frac{\tau_0}{\tau_0 + \tfrac{2}{3}} \right) \kappa_P p . \tag{A8}$$

We note several special cases of equation (A8). If $\tau_0 = 0$, we have

$$l = 2x + 4t . \tag{A9a}$$

This is just the condition one obtains by neglecting the variation of optical depth during the pulsation; it may also be obtained by a straightforward linearization of the Stefan-Boltzmann law. The condition (A9a) was used for most of the models in Paper I. A second special case is given by $\tau_0 \gg 1$:

$$l = 4x + (4 - \kappa_T)t - \kappa_P p \, . \tag{A9b}$$

This is the thermal boundary condition used for one of the models (model I_6') of Paper I. When $\tau_0 = \frac{2}{3}$, equation (A8) becomes

$$l = 3x + (4 - \tfrac{1}{2}\kappa_T)t - \tfrac{1}{2}\kappa_P p \, . \tag{A9c}$$

This is the condition actually used for all of the models of the present paper (cf. § III).

The condition (A8) may be compared with the corresponding condition derived by Unno (1964). In our notation, Unno's condition is

$$t = \tfrac{1}{4}(2n)^{(\kappa_T-4)/4}(l - 2x) + \frac{[(2n)^{(\kappa_T-4)/4} - 1]}{(\kappa_T - 4)}(l - 4x + \kappa_P p) \, , \tag{A10}$$

where

$$n = (T_0/T_e)^4 \tag{A11}$$

and T_0 is the equilibrium temperature at τ_0.

As Unno has pointed out, the difference between the correct equation (A10) and our approximate equation (A8) is apparently due to our rather crude approximation (A6) for $\langle \kappa \rangle$. In the limit $\tau_0 \gg 1$, both equations (A8) and (A10) reduce to equation (A9b). At the photosphere one must set n equal to unity in equation (A10). Depending upon the photospheric value of κ_T, the resulting expression may be quite different from equation (A9c).[2]

b) *The Mechanical Condition*

The boundary condition (21) for the mechanical quantities may be derived by supposing that the oscillations of the atmosphere obey a simple adiabatic or isothermal law. The procedure followed is to solve equations (9) and (10) with the assumption

$$\alpha p - \delta t = p/\gamma \, , \tag{A12}$$

where $\gamma = \text{const.}$ For adiabatic oscillations, $\gamma = \Gamma_1$; for isothermal oscillations, $\gamma = 1$. As Unno has shown, the thermal relaxation time of the atmospheric layers of a typical δ Cephei star is so short compared with the period that the assumption of isothermal oscillations is very good.

It is convenient to define a new independent variable:

$$z_0 = r_0/R \, . \tag{A13}$$

In terms of this variable and with the assumption (A12), equations (9) and (10) may be combined into a single second-order differential equation:

$$\frac{d^2x}{dz_0^2} + \left(\frac{4}{z_0} - \frac{R}{H_0}\right)\frac{dx}{dz_0} + \frac{R}{H_0 z_0}\left[\frac{(4 + 3\lambda\sigma^2)}{\gamma} - 3\right]x = 0 \, . \tag{A14}$$

Here we have defined the scale height

$$H_0 = R \left(\frac{d \ln P_0}{dz_0}\right)^{-1} \tag{A15}$$

and the quantity

$$\lambda = \frac{4\pi r_0^3 \bar{\rho}}{3M_r} \, . \tag{A16}$$

---

[2] The boundary conditions have also been discussed by Takeuti (1964). His treatment refines our crude treatment of the thermal condition (eqs. [A5] and [A6]) but is less general than that of Unno.

We now make the following assumptions about the equilibrium model: (i) The entire thickness of the atmosphere is small compared with the radius of the star. Thus we set $\lambda = 1$; we also put $z_0 = 1$ wherever it appears in the coefficients. This assumption also implies that the effective gravity is constant throughout the atmosphere, so that the scale height depends only on the temperature. (ii) The temperature is sufficiently low that $H_0/R \ll 1$ everywhere in the atmosphere. Thus we may neglect the first term in the coefficient of dx/dz_0. (iii) The equilibrium atmosphere is isothermal, with $T_0 = T_{\text{eff}}$. This assumption, together with (i), implies $H_0 = $ const. Equation (A14) now becomes a simple equation with constant coefficients:

$$\frac{d^2x}{dz_0{}^2} - \frac{R}{H_0}\frac{dx}{dz_0} + \frac{R}{H_0}\left[\frac{(4+3\sigma^2)}{\gamma} - 3\right]x = 0 \, . \tag{A17}$$

Upon writing, in the usual way,

$$x = \text{const. } e^{\nu z_0} \, , \tag{A18}$$

we find the two roots of equation (A17):

$$\nu_{\pm} = \frac{R}{2H_0}\left\{1 \pm \sqrt{\left[1 - \frac{4H_0}{R}\left(\frac{4}{\gamma} + \frac{3\sigma^2}{\gamma} - 3\right)\right]}\right\} \, . \tag{A19}$$

Our assumption (ii), above, assures that both roots are purely real. A general solution will then be a superposition of terms in $\exp(\nu_+ z_0)$ and $\exp(\nu_- z_0)$; by applying the additional condition that the pulsational energy of the atmosphere must remain finite as $z \to \infty$, we can eliminate the solution $\exp(\nu_+ z_0)$. Since $H_0/R \ll 1$, we have, to first order,

$$\nu_- = (4 + 3\sigma^2)/\gamma - 3 \, . \tag{A20}$$

Inserting the solution (A18) into

$$p = -\gamma\left(z_0\frac{dx}{dz_0} + 3x\right), \tag{A21}$$

which follows from equation (9), and setting $z_0 = 1$, we finally obtain

$$p = -(4 + 3\sigma^2)x \, . \tag{A22}$$

This is the mechanical boundary condition we have used. It is essentially the same as that derived by Unno from a similar but more sophisticated model. It can also be obtained from very simple physical considerations, as was done in Paper I.

c) Discussion

Some numerical tests have been carried out to investigate the effect of the choice of boundary conditions on our stability calculations. We have calculated models using condition (A9b) instead of condition (A9c), all other parameters remaining unchanged. In some cases there is a slight change in the stability coefficient; qualitatively, however, the results are not changed. More significantly, Unno (1964) investigated the effect of using the correct condition (A10) instead of our approximate condition (A9c). He also finds a small change in the stability coefficient; he points out that it is particularly the negative damping in the hydrogen ionization zone which is sensitive to the boundary condition. The deeper layers are hardly affected. Since we believe the linear approximation to be poorest in the hydrogen zone (cf. § VII), any error in the effect of this zone due to the use of poor boundary conditions may well be small compared with the error due to neglect of the non-linear effects.

In all of the tests mentioned above, the mechanical condition (A22) was used. This condition assures that no progressive waves are propagated through the atmosphere. Under certain conditions, however, this assumption might be invalid, with the consequence that mechanical energy could be lost through the photosphere. The simplest example of such a situation would be a hot

isothermal atmosphere. If T_0 is sufficiently high that H_0/R is no longer small compared with unity, then we must keep both terms in the coefficient of dx/dz_0 in equation (A14). In this case the roots ν may be complex, corresponding to running waves.

In the case of the classical Cepheids, the temperature of the photosphere is so low that the critical frequency for wave propagation is very high compared with the pulsation frequency. However, a similar effect can be produced by a corona of sufficiently high temperature and density lying above the atmosphere. It has been noted by various authors (see the discussion in Ledoux and Walraven 1958, § 68) that such running waves might have an important effect on Cepheid pulsations, particularly by increasing the mechanical damping.

In some numerical tests we applied a boundary condition based on a simple atmosphere having two isothermal layers, the upper level being hot enough to allow wave propagation. This is similar to the model investigated by Schatzman (1956). We found that, as expected, the progressive waves could have a strong damping effect due to loss of mechanical work through the photosphere. On the other hand, the positive and negative damping throughout the rest of the star was very little changed.

The problem has been considerably clarified by the investigations of Unno. His much more careful and detailed discussion confirms that progressive waves made possible by a corona can strongly damp models like those considered in this paper. He concludes, however, that the existence of a sufficiently hot and dense corona in δ Cephei stars is unlikely.

REFERENCES

Baker, N. 1963a, *Star Evolution*, ed. L. Gratton (New York: Academic Press), p. 369.
———. 1963b, "Tables of Convective Stellar Envelope Models," (NASA, Goddard Institute for Space Studies, New York) (unpublished).
———. 1965, Proc. Conference on Stellar Evolution (NASA, Goddard Institute for Space Studies, New York, November 1963) (to be published).
Baker, N., and Kippenhahn, R. 1962, *Zs. f. Ap.*, **54**, 114 (Paper I).
Christy, R. F. 1962, *Ap. J.*, **136**, 887.
———. 1964, *Rev. Mod. Phys.*, **36**, 555.
Cox, J. P. 1960, *Ap. J.*, **132**, 594.
———. 1963, *ibid.*, **138**, 487 (C63).
———. 1965, Proc. Conference on Stellar Evolution (NASA, Goddard Institute for Space Studies, New York November 1963) (to be published).
Epstein, I. 1950, *Ap. J.*, **112**, 6.
Henyey, L. G., Forbes, J. E., and Gould, N. L. 1964, *Ap. J.*, **139**, 306.
Hofmeister, E., Kippenhahn, R., and Weigert, A. 1964a, *Zs. f. Ap.*, **59**, 115 (HKW I).
———. 1964b, *ibid.*, p. 242 (HKW II).
———. 1964c, *ibid.*, **60**, 57 (HKW III).
———. 1965, Proc. Conference on Stellar Evolution (NASA, Goddard Institute for Space Studies, New York, November 1963) (to be published).
Ledoux, P. 1963, *Star Evolution*, ed. L. Gratton (New York: Academic Press), p. 394.
Ledoux, P., and Walraven, Th. 1958, *Hdb. d. Phys.*, ed. S. Flügge (Berlin: Springer-Verlag), **51**, 353.
Oke, J. B. 1961, *Ap. J.*, **133**, 90.
Osawa, K. 1956, *Ap. J.*, **123**, 513.
Schatzman, E. 1956, *Ann. d'ap.*, **19**, 45.
Takeuti, M. 1964, *Pub. Astr. Soc. Japan*, **16**, 64.
Temesvary, St. 1964, unpublished.
Unno, W. 1964, to be published.
Unsöld, A. 1955, *Physik der Sternatmosphären*, 2. Aufl. (Berlin: Springer-Verlag), Sec. 51.
Zhevakin, S. A. 1963, *Ann. Rev. Astr. and Ap.*, **1**, 367.